a frequency corresponding to the plunge resonance. For the closed-loop, nonlinear system, the dominant LCO frequency is approximately that of the flap resonance. The primary effect of the dynamic compensator serves to convert the high-amplitude, low-frequency LCOs of the nonlinear system to low-amplitude, high-frequency LCOs.

Acknowledgment

The authors gratefully acknowledge the Air Force Office of Scientific Research for funding this research under Grant F49620-96-1-0385, monitored by Maj. Brian Sanders.

References

[1]Vipperman, J. S., Clark, R. L., Conner, M., and Dowell, E. H., "Investigation of the Experimental Active Control of a Typical Section Airfoil Using a Trailing Edge Flap," *Journal of Aircraft*, Vol. 35, No. 2, 1998, pp. 224–229.

[2]Vipperman, J. S., Barker, J. M., Clark, R. L., and Balas, G. J., "Comparison of μ- and $\mathcal{H}_2$-Synthesis Controllers on an Experimental Typical Section," *Journal of Guidance, Control, and Dynamics*, Vol. 22, No. 2, 1999, pp. 278–285.

[3]Frampton, K. D., and Clark, R. L. , "Experiments on Control of Limit Cycle Oscillations in a Typical Section," *Journal of Guidance, Control, and Dynamics* (to be published).

[4]Conner, M. D., Tang, D. M., Dowell, E. H., and Virgin, L. N., "Nonlinear Behavior of a Typical Airfoil Section with Control Surface Freeplay: A Numerical and Experimental Study," *Journal of Fluids and Structures*, Vol. 11, No. 1, 1997, pp. 89–109.

[5]Edwards, J. W., Ashley, H., and Breakwell, J. V., "Unsteady Aerodynamic Modeling for Arbitrary Motions," *AIAA Journal*, Vol. 17, No. 4, 1979, pp. 365–374.

Modification of a Helicopter Inverse Simulation to Include an Enhanced Rotor Model

Sharon A. Doyle* and Douglas G. Thomson†
Glasgow University,
Glasgow, Scotland G12 8QQ, United Kingdom

Nomenclature

h	= maximum maneuver height, m
I_R	= effective inertia of the main rotor, kg · m^2
K_3	= engine model gain
k	= current solution time point
n_{pts}	= number of points in inverse simulation/maneuver
Q_E	= engine torque, N · m
Q_R	= main rotor torque, N · m
Q_{TR}	= tail rotor torque, N · m
Q_{tr}	= transmission torque, N · m
r	= fuselage yaw rate, rad/s
t	= time, s
t_k	= time point in inverse simulation/maneuver definition
t_m	= time taken to complete a maneuver, s
$\boldsymbol{u}$	= control vector
V_f	= aircraft flight velocity, m/s
x_e, y_e, z_e	= displacements relative to an Earth-fixed inertial frame, m
$\boldsymbol{y}$	= output vector
$\boldsymbol{y}_{\text{des}}$	= desired output vector
Δt	= inverse simulation/maneuver discretization interval, s
θ_0	= main rotor collective pitch angle, rad
$\theta_{0\text{tr}}$	= tail rotor collective pitch angle, rad
θ_{1s}, θ_{1c}	= main rotor longitudinal and lateral cyclic pitch angles, rad
τ_{e1}, τ_{e2}, τ_{e3}	= engine time constants, s
ψ	= heading, rad
ψ_{azi}	= blade azimuth angle, rad
Ω	= main rotorspeed, rad/s
Ω_i	= idling rotorspeed, rad/s

Received 26 March 1999; revision received 21 September 1999; accepted for publication 21 September 1999.

*Postgraduate Research Student, Department of Aerospace Engineering, James Watt Building.

†Senior Lecturer, Department of Aerospace Engineering, James Watt Building.

I. Introduction

AN individual blade rotor model has been developed at the University of Glasgow by Rutherford and Thomson[1] for use in helicopter inverse simulation. In the context of helicopter flight dynamics, an inverse simulation generates the control time histories for the modeled helicopter performing a defined task. To implement such a model in an inverse sense, it is necessary to adopt a numerical integration technique similar to that proposed by Hess et al.[2] The generic inverse simulation algorithm (Genisa) used by Rutherford and Thomson is described in detail in Ref. 1, where the problem of numerical stability is also addressed.

The helicopter individual blade rotor model (Hibrom) represents the state of the art in helicopter inverse simulation. Some simplifying assumptions were made in its development; the most significant of which is the assumption of constant rotorspeed (see Ref. 1; Conclusions). It is important to model this degree of freedom because it has a direct influence on the dynamic behavior of the main rotor. In addition, the inclusion of the rotorspeed degree of freedom must be achieved before other modeling features, such as lead/lag freedom, can be incorporated. This Engineering Note describes modifications made to the inverse algorithm Genisa that allow the rotorspeed degree of freedom to be incorporated within Hibrom.

II. Genisa

The integration-based inverse solver Genisa is essentially a modification of that documented by Hess et al.[2] and is driven by specified maneuver constraints. The starting point is, therefore, a mathematical definition of the desired flight path to be followed by the subject vehicle. Genisa operates by constraining the helicopter's Earth-referenced accelerations along with one attitude (heading in the case of a longitudinal maneuver), and so the desired output vector $\boldsymbol{y}_{\text{des}}$ is evaluated for a series of n_{pts} discrete time points:

$$\boldsymbol{y}_{\text{des}}(t_k) = \{\ddot{x}_e(t_k) \quad \ddot{y}_e(t_k) \quad \ddot{z}_e(t_k) \quad \dot{\psi}(t_k)\}^T$$

$$0 \le t_k \le t_m, \quad k = 1, n_{\text{pts}} \qquad (1)$$

The altitude $z_e(t_k)$ is specified as a polynomial function of time.

The Genisa algorithm then proceeds by making an initial estimate of the applied control inputs that, over a predefined time increment, will result in the helicopter having the desired accelerations and heading. These control displacements are applied to the helicopter model, and the equations of motion are solved by numerical integration to obtain the helicopter's actual states at the next time point. An iterative scheme is then set up whereby control displacements are adjusted until the error between desired and actual outputs is within a prescribed tolerance. This process is repeated for each time interval, yielding a control time history $\boldsymbol{u}(t_k)$ for the complete maneuver, where

$$\boldsymbol{u}(t_k) = \{\theta_0(t_k) \quad \theta_{1s}(t_k) \quad \theta_{1c}(t_k) \quad \theta_{0\text{tr}}(t_k)\}^T \qquad (2)$$

The success of the method just outlined relies on the selection of a suitable time step Δt, over which the applied controls are to be held constant. The rotor forces and moments are calculated by integrating elemental forces over the span of each blade. Because the velocity at each spanwise location varies as the blade rotates, the total force calculated is harmonic with period equal to a complete revolution of the blade (or $1/n$ revolutions of an n-bladed rotor). For

the Genisa/Hibrom inverse simulation, the time step is, therefore, chosen to match an integer number of main rotor periods, thereby accommodating the rotor periodicity that is inherent in the individual blade rotor model. Unfortunately, this requires the assumption of constant rotorspeed to be made. In the following section, modifications to the Genisa algorithm will be described that eliminate the necessity to constrain rotorspeed, thereby allowing an engine governor model to be included in Hibrom.

III. Enhanced Genisa/Hibrom Inverse Simulation

A. Description of the Engine Governor Model

Variations in rotorspeed due to changes in torque demand are sensed by an engine governor. The governor then attempts to redress the imbalance by demanding a suitable change in fuel flow, thereby increasing or decreasing the engine torque output as required. Naturally there is a lag between the rotorspeed change and the resulting torque change, and hence, the rotorspeed is a degree of freedom within the system. Hibrom has been modified to include a simple model of the engine governor that is essentially that given by Padfield[3] and is described briefly here.

Rotorspeed Ω is related to the engine torque output Q_E by the equation

$$\dot{\Omega} = (1/I_R)(Q_E - Q_R - Q_{\mathrm{TR}} - Q_{\mathrm{tr}}) + \dot{r} \tag{3}$$

The overall engine torque response to a change in rotorspeed is then given by the second-order, nonlinear differential function

$$\ddot{Q}_E = (1/\tau_{e1}\tau_{e3})[-(\tau_{e1} + \tau_{e3})\dot{Q}_E - Q_E + K_3(\Omega - \Omega_i + \tau_{e2}\dot{\Omega})] \tag{4}$$

The lead and lag time constants, τ_{e2} and τ_{e3}, are in fact functions of engine torque, introduced in transfer functions representing the demanded fuel flow change in response to a change in rotorspeed and the resulting engine torque response. Equations (3) and (4) are now included in the main rotor model Hibrom, resulting in three additional degrees of freedom corresponding to Ω, Q_E, and $\dot{Q}_E$.

B. Modifications to Genisa

As discussed in Sec. II, the periodic nature of the rotor forcing requires that the solution time interval matches an integer number of main rotor periods, that is, a quarter turn for a four-bladed rotor. Assuming constant rotorspeed, this interval can be conveniently fixed throughout the simulation. The existing Genisa algorithm typically requires a time consistent with one-half turn of the main rotor, which Rutherford[4] found to be "sufficiently long to allow the transient dynamics to settle." Once this discretization interval has been established, the desired output can be calculated at each time point and used as input to Genisa.

With the introduction of the rotorspeed degree of freedom, the period of the main rotor is no longer fixed, and hence, the solution interval must vary throughout the simulation. Consequently, the desired flight path can no longer be determined independently of the main program, and the time required to complete the maneuver will not be known a priori.

This problem is overcome by expanding the control vector $\boldsymbol{u}(t_k)$ to include an estimate of the next time point that will allow sufficient time for the rotor blades to sweep out the desired azimuth. Similarly, the output vector $\boldsymbol{y}(t_k)$ will now include blade azimuth. The augmented control and output vectors are then given by

$$\boldsymbol{u}(t_k) = \{\theta_0(t_k) \quad \theta_{1s}(t_k) \quad \theta_{1c}(t_k) \quad \theta_{0\mathrm{tr}}(t_k) \quad t_{k+1}\}^T \tag{5}$$

$$\boldsymbol{y}(t_k) = \{\ddot{x}_e(t_k) \quad \ddot{y}_e(t_k) \quad \ddot{z}_e(t_k) \quad \dot{\psi}(t_k) \quad \psi_{\mathrm{azi}}(t_k)\}^T \tag{6}$$

The next time point t_{k+1} is determined such that the error between the actual and desired blade azimuth is minimized.

When the rotorspeed was fixed, the maneuver time t_m was chosen to coincide with a whole number of rotor periods. With the rotor period no longer held constant, the procedure is to estimate the total maneuver time t_m, thereafter evaluating the desired output vector at each time point in turn, until t_m has been exceeded. The rotor model is, therefore, enhanced by including an engine governor model and, hence, the rotorspeed degree of freedom, at the expense of a small loss of accuracy in the maneuver definition.

IV. Results

The enhanced individual blade rotor model with rotorspeed degree of freedom has been validated against flight data for a quick-hop maneuver. The results of this validation exercise are not presented because they are very similar to those previously documented in Ref. 1. In both cases, the simulation successfully captures the overall trend in each variable, although some peak values are significantly underpredicted. A more detailed discussion of the validation process can be found in Ref. 1.

To ensure that the new algorithm has been implemented correctly, results can be obtained with the engine equations (3) and (4) disabled. The rotorspeed and engine states, Ω, Q_E, and $\dot{Q}_E$, are, thus, constrained, isolating the operation of the new algorithm from any modifications made to the model. It was confirmed in this way that changes made to the existing algorithm do not affect the verity of the solution.

With some confidence in the validity of the rotor model and confirmation that the algorithm is operating satisfactorily, it is now possible to examine the effect of including rotorspeed as a degree of freedom within the modeled system. The inverse simulation of a hurdle-hop maneuver is considered whereby the pilot's task is to clear a 5-m-high obstacle and return to the original altitude over a distance of 150 m. A constant forward speed of 40 kn is maintained, and the obstacle is assumed to be located at the midpoint of the maneuver. The results in Figs. 1 and 2 are compared directly with those obtained using the original Hibrom model without the rotorspeed degree of freedom. The two sets of results are qualitatively similar, although the addition of an engine governor model with the rotorspeed degree of freedom has clearly influenced the magnitude of the controls. The new Genisa/Hibrom inverse simulation predicts a greater range of control movements necessary to fly the specified maneuver and it may be expected that a greater difference between the two sets of results will be observed for more severe maneuvers.

In the results shown a solution time interval corresponding to two turns of the main rotor was used, $\Delta t_k = 4\pi/\Omega_k$. When the frequency of control application is increased to once per revolution of the main rotor, the results deteriorate, with unstable oscillations developing in the lateral cyclic control and engine torque derivative. Furthermore, the simulation will not perform with a solution interval corresponding to one-half turn of the rotor. The most likely explanation of this

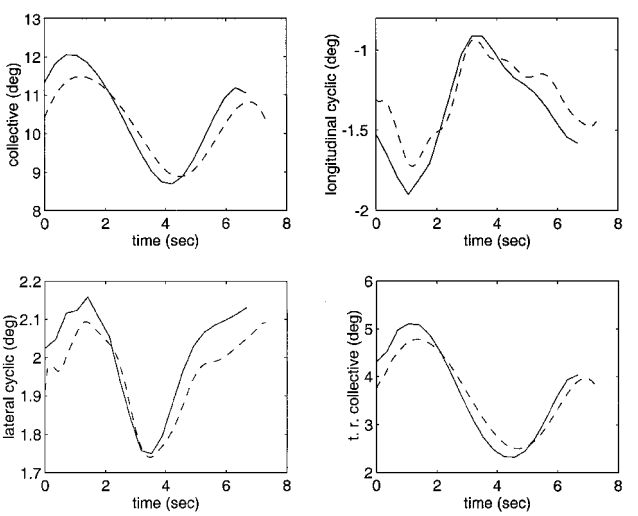

Fig. 1 Comparison between inverse simulation results generated by Genisa/Hibrom I and II (hurdle hop: V_f = 40 kn, h = 5 m, s = 150 m); time step: two turns of main rotor. ——, Genisa/Hibrom II, and – – –, Genisa/Hibrom I.

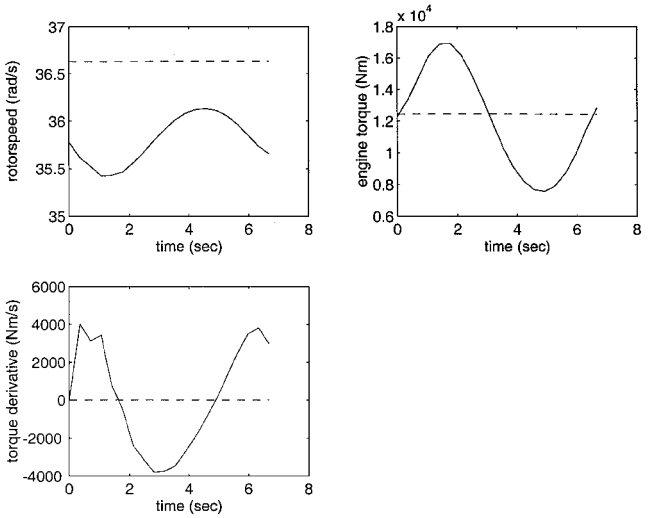

Fig. 2 Comparison between inverse simulation results generated by Genisa/Hibrom I and II (hurdle hop: V_f = 40 kn, h = 5 m, s = 150 m); time step: two turns of main rotor. ——, Genisa/Hibrom II, and – – –, Genisa/Hibrom I.

behavior is that a minimum interval corresponding to two turns of the main rotor is required to allow the transient engine dynamics to settle down toward a new steady state following each application of the controls. The time constant associated with a first-order approximation to the engine governor model is typically 0.397 s. This is more than double the time interval of 0.1755 s that corresponds to one full turn of the main rotor. This explanation can be verified by reducing the engine model time constants τ_{e1}, τ_{e2}, and τ_{e3} to 1% of their nominal values. The results improve, and a control application interval of once per revolution produces smooth control time histories and engine states.

V. Conclusions

An engine governor model has been successfully incorporated into the individual blade rotor model Hibrom for helicopter inverse simulation. Hence, the rotorspeed is now a degree of freedom within the modeled system.

A series of modifications have been made to the solution algorithm Genisa to accommodate the variation in rotorspeed. In particular, the control application interval is now recalculated iteratively at each time step. This is necessary to match the rotor periodicity that is inherent in the individual blade rotor model. In addition, the control application interval must be sufficiently long to allow the transient dynamics to settle; otherwise algorithm failure can occur.

The addition of the rotorspeed degree of freedom does not significantly affect the predicted control time histories for the maneuver considered in this study. However, as the boundaries of the flight envelope are approached, it may be expected that the enhanced rotor model will be closer to predicting actual flight behavior. Furthermore, with the introduction of the rotorspeed degree of freedom, it will now be possible to improve simulation fidelity by including other blade degrees of freedom.

References

[1]Rutherford, S., and Thomson, D. G., "Helicopter Inverse Simulation Incorporating an Individual Blade Rotor Model," *Journal of Aircraft*, Vol. 34, No. 5, 1997, pp. 627–634.

[2]Hess, R. A., Gao, C., and Wang, S. H., "Generalized Technique for Inverse Simulation Applied to Aircraft Maneuvers," *Journal of Guidance, Control, and Dynamics*, Vol. 14, No. 5, 1991, pp. 920–926.

[3]Padfield, G. D., "A Theoretical Model of Helicopter Flight Mechanics for Application to Piloted Simulation," Royal Aircraft Establishment, TR 81048, Bedford, England, U.K., April 1981.

[4]Rutherford, S., "Simulation Techniques for the Study of the Manoeuvring of Advanced Rotorcraft Configurations," Ph.D. Dissertation, Dept. of Aerospace Engineering, Univ. of Glasgow, Glasgow, Scotland, U.K., March 1997.

Structural Dynamics and Quasistatic Aeroelastic Equations of Motion

John R. Dykman* and William P. Rodden†
The Boeing Company, Long Beach, California 90807-5309

Introduction

THE quasistatic aeroelastic equations of motion of a flight vehicle include all of the static effects of flexibility and assume that there are no structural dynamic effects, i.e., the vehicle is regarded a point vehicle with six degrees of freedom. Thus, all points of the structure are in phase with the motions of a reference point, e.g., the center of gravity or the quarter point of the mean aerodynamic reference chord. The dynamic effects of structural modes cannot be included simply by adding the modal equations of motion to couple with the quasistatic equations, as has been incorrectly suggested by Rodden and Love.[1] The correct formulation begins with the mean axis equations of motion to which the modal dynamic equations are added with all appropriate aeroelastic coupling.[2] Many modes must be included to account accurately for static aeroelastic behavior, but because not all of these are necessary to account for the dynamic response, the high-frequency modes can be eliminated by residualization.[3]

Residualization of the Aeroelastic Equations of Motion

The fundamental equation of motion of a linear aeroelastic system in generalized (modal) coordinates is given in Eq. (1). The system free vibration mode shapes are the generalized coordinates $\boldsymbol{q}$ and the control surface inputs are generalized coordinates $\boldsymbol{q}^c$.

$$\boldsymbol{M}\ddot{\boldsymbol{q}} + \boldsymbol{C}\dot{\boldsymbol{q}} + \boldsymbol{K}\boldsymbol{q} = \bar{q}\boldsymbol{Q}_0(M) + \mathcal{F}^{-1}[\bar{q}\boldsymbol{Q}(M,k)\boldsymbol{q}] - \boldsymbol{M}^c\ddot{\boldsymbol{q}}^c + \mathcal{F}^{-1}[\bar{q}\boldsymbol{Q}^c(M,k)\boldsymbol{q}^c] + \boldsymbol{W} \tag{1}$$

The generalized structural mass, damping, and stiffness matrices are $\boldsymbol{M}$, $\boldsymbol{C}$, and $\boldsymbol{K}$, respectively; $\boldsymbol{W}$ is a vector of weight and static unbalance components adjusted for the trim pitch angle of the mean axes. The coupled control surface generalized structural mass matrix is $\boldsymbol{M}^c$, and the control surface stiffness and damping are neglected. The generalized aerodynamic coefficients $\boldsymbol{Q}_0(M)$ are intercept values for incidence, twist, and camber and are functions of the Mach number M. The generalized unsteady aerodynamic coefficients $\boldsymbol{Q}(M,k)$ and the coupled control surface generalized unsteady aerodynamic coefficients $\boldsymbol{Q}^c(M,k)$ in the frequency domain are functions of Mach number and reduced frequency k, where $k = \omega\bar{c}/2V$ in which ω is the angular frequency, $\bar{c}$ is the reference chord, and V is the flight velocity. The aerodynamic force is scaled by dynamic pressure $\bar{q}$, where $\bar{q} = \rho V^2/2$ in which ρ is the atmospheric density. $\mathcal{F}^{-1}[\,]$ represents the inverse Fourier transform of the quantity in brackets. The generalized unsteady aerodynamic coefficients are complex and can be separated into their real and imaginary parts to obtain an approximation in the time domain as

$$\mathcal{F}^{-1}[\bar{q}\boldsymbol{Q}(M,k)\boldsymbol{q}] = \mathcal{F}^{-1}\{\bar{q}[{}^R\boldsymbol{Q}(M,k)]\boldsymbol{q} + \bar{q}(\bar{c}/2V)[{}^I\boldsymbol{Q}(M,k)/k]i\omega\boldsymbol{q}\} \approx \bar{q}\boldsymbol{A}\boldsymbol{q} + \bar{q}(\bar{c}/2V)\boldsymbol{B}\dot{\boldsymbol{q}} \tag{2}$$

The coefficients are obtained from an unsteady aerodynamic theory such as the doublet-lattice method,[4,5] where $\boldsymbol{A}$ is the real part of the generalized aerodynamic force (GAF) matrix and $\boldsymbol{B}$ is the imaginary

Received 7 July 1998; revision received 26 November 1999; accepted for publication 23 January 2000.

*Principal Engineer of Stability, Control, and Flying Qualities. Member AIAA.

†Consultant.